J Biol Inorg Chem (2005) 10: 87–93
DOI 10.1007/s00775-005-0624-x

MINIREVIEW

Kevin D. Koehntop · Joseph P. Emerson
Lawrence Que Jr

The 2-His-1-carboxylate facial triad: a versatile platform for dioxygen activation by mononuclear non-heme iron(II) enzymes

Received: 24 November 2004 / Accepted: 4 January 2005 / Published online: 1 March 2005

Abstract General knowledge of dioxygen-activating mononuclear non-heme iron(II) enzymes containing a 2-His-1-carboxylate facial triad has significantly expanded in the last few years, due in large part to the extensive library of crystal structures that is now available. The common structural motif utilized by this enzyme superfamily acts as a platform upon which a wide assortment of substrate transformations are catalyzed. The facial triad binds a divalent metal ion at the active site, which leaves the opposite face of the octahedron available to coordinate a variety of exogenous ligands. The binding of substrate activates the metal center for attack by dioxygen, which is subsequently converted to a high-valent iron intermediate, a formidable oxidizing species. Herein, we summarize crystallographic and mechanistic features of this metalloenzyme superfamily, which has enabled the proposal of a common but flexible pathway for dioxygen activation.

Keywords α-Ketoglutarate dependent enzymes · 2-His-1-carboxylate facial triad · Extradiol-cleaving catechol dioxygenases · Pterin-dependent hydroxylases · Rieske dioxygenases

Abbreviations α-KG: α-Ketoglutarate · 2,3-CTD: Catechol 2,3-dioxygenase · 4,5-PCD: Protocatechuate 4,5-dioxygenase · A1: Deoxyguanidinoprocla-vaminate · ACCO: 1-Aminocyclopropane-1-carboxylic acid oxidase · ACV: δ-(L-α-Aminoadipoyl)-L-cysteinyl-D-valine · ANS: Anthocyanidin synthase · AtsK: Alkylsulfatase · BH_4: 6(*R*)-L-*erythro*-5,6,7,8-Tetrahydrobiopterin · BphC: 2,3-Dihydroxybiphenyl 1,2-dioxygenase · CarC: Carbapenem synthase · CAS: Clavaminate synthase · DAOCS: Deacetoxycepha-losporin C synthase · DFT: Density functional theory · DHBD: Synonymous with BphC · DHBP: 2,3-Dihydroxybiphenyl · EXAFS: Extended X-ray absorption fine structure · FIH-1: Factor-inhibiting hypoxia-inducible factor-1 · HGO: Homogentisate 1,2-dioxygenase · HPCD: Homoprotocatechuate 2,3-dioxygenase · HPPD: 4-Hydroxyphenylpyruvate dioxygenase · IPNS: Isopenicillin *N* synthase · LigAB: Synonymous with 4,5-PCD · MCD: Magnetic circular dichroism · MndD: Mn^{II}-dependent HPCD · MPC: Metapyrocatechase (synonymous with 2,3-CTD) · NDO: Naphthalene 1,2-dioxygenase · PCV: Proclavaminate · PheOH: Phenylalanine hydroxylase · TauD: Taurine/α-KG dioxygenase · THA: 3-(2-Thienyl)-L-alanine · TrpOH: Tryptophan hydroxylase · TyrOH: Tyrosine hydroxylase

K. D. Koehntop · J. P. Emerson · L. Que Jr (✉)
Department of Chemistry and Center for Metals in Biocatalysis, University of Minnesota, Minneapolis, MN 55455, USA
E-mail: que@chem.umn.edu
Fax: +1-612-6247029

Introduction

Nature typically employs metal centers within enzymes to activate molecular oxygen, carrying out crucial transformations involved in metabolism, mammalian physiology, and biodegradation processes [1–9]. A specific subset of these enzymes consists of those having mononuclear non-heme iron(II) active sites that catalyze a wide variety of reactions, including the hydroxylation of aliphatic C–H bonds, the epoxidation of C–C double bonds, the *cis*-dihydroxylation of arene double bonds, heterocyclic ring formation, and oxidative aromatic ring cleavage. These reactions appear to represent a range of substrate transformations that is even broader than that associated with oxidative heme enzymes [10].

Crystallographic data on this superfamily of enzymes (Table 1) accumulated only within the past 10 years [11–20] have established the occurrence of a common structural motif that binds the divalent iron center, coined the 2-His-1-carboxylate facial triad [21, 22]. This motif consists of three endogenous protein ligands arranged at the vertices of one triangular face of an

Table 1 Crystallographically characterized mononuclear non-heme Fe^{II} enzymes containing a 2-His-1-carboxylate facial triad

Enzyme type	Crystallized enzyme (PDB code)	Sequence motif	Structure motif
Extradiol cleaving catechol dioxygenases	**BphC** [or **DHBD**] (1DHY, 1EIL, 1EIQ, 1EIR, 1KW3, 1KW6, 1KW8, 1KW9, 1KWB, 1KWC)[a] (1HAN, 1KMY, 1KND, 1KNF, 1LGT, 1LKD)[b]	**H**X_{63}**H**X_{50}**E** **H**X_{63}**H**X_{49}**E**	$\beta\alpha\beta_3$ modules [11]
	2,3-CTD [or **MPC**] (1MPY)[c]	**H**X_{60}**H**X_{50}**E**	
	HPCD (1F1X, 1Q0C, 1Q0O)[d]	**H**X_{58}**H**X_{52}**E**	
	MndD[e] (1F1R, 1F1U, 1F1V)[f]		
	4,5-PCD [or **LigAB**] (1B4U, 1BOU)[g]	**H**X_{48}**H**X_{180}**E**	α: plate-like; β: α/β [57]
	HGO (1EY2, 1EYB)[h]	**H**X_5**E**X_{29}**H**	Jelly roll [58]
Rieske dioxygenases	**NDO** (1EG9, 1NDO, 1O7G, 1O7H, 1O7M, 1O7N, 1O7P, 1O7W)[a]	**H**X_4**H**X_{148}**D**	α (N-terminus): β-sheet; α (C-terminus): antiparallel β-pleated sheet; β: twisted mixed β-sheet [17]
α-KG dependent enzymes	**ANS** (1GP4, 1GP5, 1GP6)[i]	**HXD**X_{53}**H**	Jelly roll [15]
	AtsK (1OIH, 1OII, 1OIJ, 1OIK, 1VZ4, 1VZ5)[c]	**HXD**X_{153}**H**	
	TauD (1GQW, 1GY9, 1OS7, 1OTJ)[j]		
	CarC (1NX4, 1NX8)[k]	**HXD**X_{147}**H**	
	CAS (1DRT, 1DRY, 1DS0, 1DS1, 1GVG)[l]	**HXE**X_{132}**H**	
	DAOCS (1DCS, 1E5H, 1E5I, 1HJF, 1HJG, 1RXF, 1RXG, 1UNB, 1UO9, 1UOB, 1UOF, 1UOG, 1W28, 1W2A, 1W2N, 1W2O)[l]	**HXD**X_{57}**H**	
	FIH-1 (1H2K, 1H2L, (1H2M)[m], 1H2N, 1IZ3, 1MZE, 1MZF)[h]	**HXD**X_{77}**H**	
	Gab (1JR7)[j]	**HXD**X_{129}**H**	
	Proline 3-hydroxylase (1E5R, 1E5S)[n]	**HXD**X_{48}**H**	
	HPPD (1CJX)[o] (1SP8)[p] (1SP9, 1SQD, 1TFZ, 1TG5)[i] (1SQI)[q] (1T47)[r]	**H**X_{78}**H**X_{81}**E** **H**X_{81}**H**X_{85}**E** **H**X_{82}**H**X_{82}**E** **H**X_{82}**H**X_{78}**E**	$\beta\alpha\beta_3\alpha$ modules [59]
Pterin dependent hydroxylases	**PheOH** (1DMW, 1J8T, 1J8U, 1KW0, 1LRM, 1MMK, 1MMT, 1PAH, 2PAH, 3PAH, 4PAH, 5PAH, 6PAH)[h] (1PHZ, 2PHM)[q]	**H**X_4**H**X_{39}**E**	Catalytic: α-helical basket; Tetramerization: antiparallel coiled coil [60]; Regulatory: α-β sandwich [61]
	TrpOH (1MLW)[h]		
	TyrOH (1TOH, 2TOH)[q]		
	PheOH (1LTU, 1LTV, 1LTZ)[s]	**H**X_4**H**X_{40}**E**	α-helical basket [62]
Other oxidases	**IPNS** (1BK0, 1BLZ, 1HB1, 1HB2, 1HB3, 1HB4, (1IPS),[t] 1OBN, 1OC1, 1ODM, 1ODN, 1QIQ, 1QJE, 1QJF)[u] (1UZW)[v]	**HXD**X_{53}**H**	Jelly roll [13]
	ACCO[w]	**HXD**X_{54}**H**	Jelly roll [20]

α-KG α-ketoglutarate, *BphC* and *DHBD* 2,3-dihydroxybiphenyl 1,2-dioxygenase, *2,3-CTD* catechol 2,3-dioxygenase, *MPC* metapyrocatechase, *HPCD* homoprotocatechuate 2,3-dioxygenase, *MndD* Mn^{II}-dependent HPCD, *4,5-PCD* and *LigAB* protocatechuate 4,5-dioxygenase, *HGO* homogentisate 1,2-dioxygenase, *NDO* naphthalene 1,2-dioxygenase, *ANS* anthocyanidin synthase, *AtsK* alkylsulfatase, *TauD* taurine/α-KG dioxygenase, *CarC* carbapenem synthase, *CAS* clavaminate synthase, *DAOCS* deacetoxycephalosporin C synthase, *FIH-1* factor-inhibiting hypoxia-inducible factor-1, *HPPD* 4-hydroxyphenylpyruvate dioxygenase, *PheOH* phenylalanine hydroxylase, *TrpOH* tryptophan hydroxylase, *TyrOH* tyrosine hydroxylase, *IPNS* isopenicillin *N* synthase, *ACCO* 1-aminocyclopropane-1-carboxylic acid oxidase

[a]From *Pseudomonas* sp. [b]From *Burkholderia* sp. [c]From *Pseudomonas putida*. [d]From *Brevibacterium fuscum*. [e]Mn^{II}-dependent. [f]From *Arthrobacter globiformis*. [g]From *Sphingomonas paucimobilis*. [h]From *Homo sapiens*. [i]From *Arabidopsis thaliana*. [j]From *Escherichia coli*. [k]From *Erwinia carotovora*. [l]From *Streptomyces clavuligerus*. [m]Zn^{II} complex. [n]From *Streptomyces* sp. [o]From *Pseudomonas fluorescens*. [p]From *Zea mays*. [q]From *Rattus norvegicus*. [r]From *Streptomyces avermitilis*. [s]From *Chromobacterium violaceum*. [t]Mn^{II} complex. [u]From *Aspergillus nidulans*. [v]From *Emericella nidulans*. [w]From *Petunia hybrida*. The PDB files corresponding to the ACCO structures were not available when this article was published.

octahedron, which anchor the iron to the enzyme (Fig. 1). This three-pronged mode of attachment is in contrast to that for heme enzymes, which, by their very nature, must have the four equatorial sites occupied by the porphyrin. One axial site is then occupied by a variable amino acid residue that affixes the metalloporphyrin in the active site; this leaves only one coordination site available for an exogenous ligand, which must be dioxygen or one of its reduced derivatives. On the other hand, the metal centers of the non-heme iron enzymes have three coordination sites opposite the 2-His-1-carboxylate facial triad available for binding exogenous ligands such as O_2, substrate, and/or cofactor that provide the protein with the flexibility with which to tune the reactivity of the iron(II) center.

The 2-His-1-carboxylate facial triad thus serves as a versatile platform for dioxygen activation. An impressive assortment of substrate transformations is catalyzed by a diverse collection of mononuclear non-heme iron(II) enzymes with distinct requirements for catalysis. Accordingly, they have been classified into five families in Fig. 2. The extradiol-cleaving catechol dioxygenases

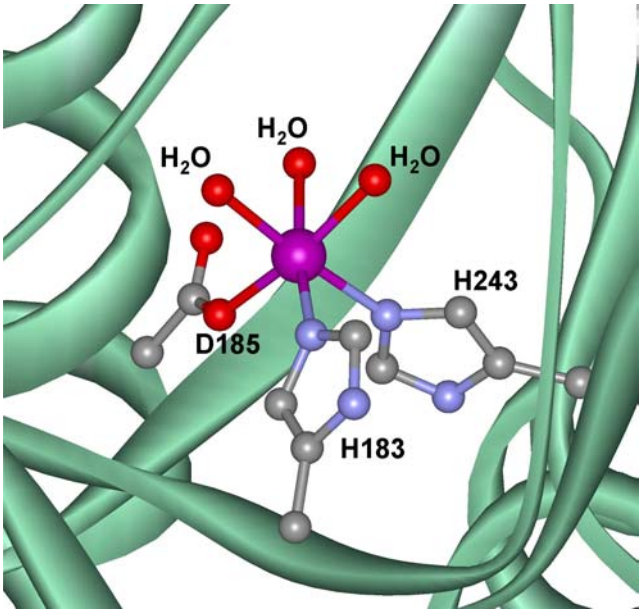

Fig. 1 The 2-His-1-carboxylate facial triad exemplified by the resting state of deacetoxycephalosporin C synthase (DAOCS), an α-ketoglutarate (α-KG) dependent mononuclear non-heme iron enzyme (1RXF.pdb)

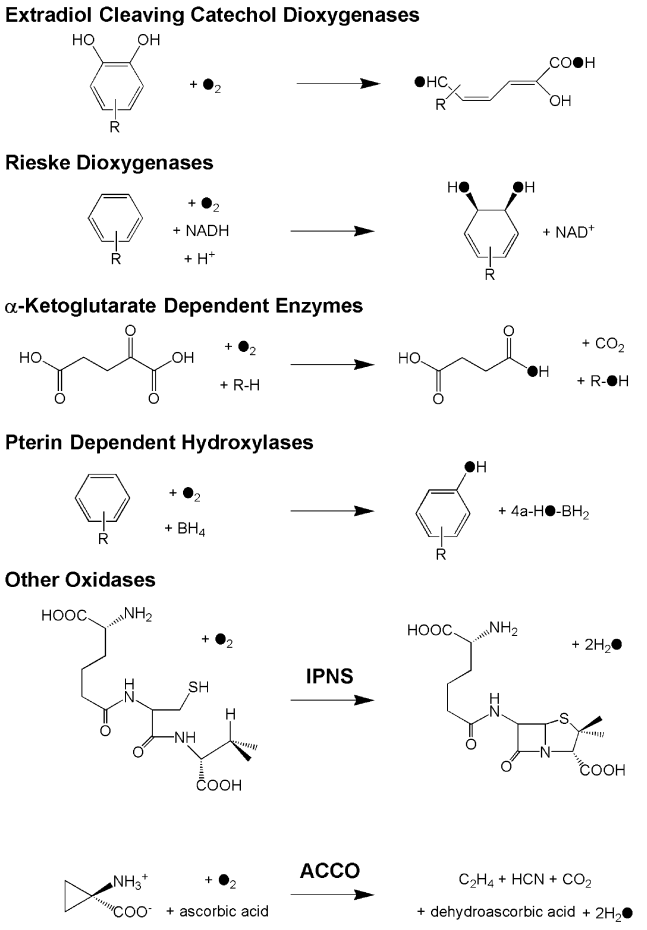

Fig. 2 Reactions catalyzed by each of the five families of mononuclear non-heme iron enzymes containing a 2-His-1-carboxylate facial triad. Dioxygen is labeled to display the fate of each oxygen atom

catalyze the aromatic ring cleavage of catechols at the C–C bond adjacent to the enediol group via a four-electron oxidation that incorporates both atoms of dioxygen into the product [6]. Rieske dioxygenases catalyze the *cis*-dihydroxylation of an arene double bond in which NADH serves as the two-electron source; furthermore both atoms of O_2 are incorporated into the substrate, forming a *cis*-diol product [5]. The third class represents a remarkably versatile group of enzymes that require as the electron source a 2-oxoacid cosubstrate, typically α-ketoglutarate (α-KG), which undergoes oxidative decarboxylation during the reaction. The oxidizing equivalents produced therefrom can be used to effect C–H hydroxylation, oxygen-atom transfer, heterocyclic ring formation, or desaturation reactions [8, 9]. In yet another class are the aromatic amino acid hydroxylases, which utilize the tetrahydrobiopterin cofactor (BH_4) as the electron source to hydroxylate the rings of aromatic amino acid residues; these enzymes are responsible for the rate-determining step in the formation of the neuronal signaling agents serotonin and the catecholamines [6, 7]. The last group represents a "catch-all" category for oxidases that at present includes isopenicillin *N* synthase (IPNS) [23], the ethylene-forming enzyme 1-aminocyclopropane-1-carboxylic acid oxidase (ACCO) [20, 24–26], and fosfomycin epoxidase [27, 28].

Not surprisingly, extensive primary sequence homology exists within each family of mononuclear non-heme iron(II) enzymes containing a 2-His-1-carboxylate facial triad (Table 1) [13, 29–35]. However, these sequence motifs differ among the families, suggesting a convergent evolutionary pattern that has favored this structural motif. Herein, we summarize structural features of the active sites from these five families of dioxygen-activating mononuclear iron enzymes that reveal a common but flexible mechanism for dioxygen activation.

Active site structures

There are currently an astounding number of X-ray crystal structures available for dioxygen-activating mononuclear non-heme iron(II) enzymes (more than 125 structures of 30 different enzymes as of January 2005). These structures, some of which reflect a single enzyme at different stages of its catalytic cycle, definitively establish the 2-His-1-carboxylate facial triad as the common active site motif for all five enzyme families. The active site of a resting enzyme is exemplified by the α-KG dependent enzyme deacetoxycephalosporin C synthase (DAOCS, Fig. 1). On one face of this octahedral metal center is the 2-His-1-carboxylate triad, a monoanionic ligand set for binding iron(II), with

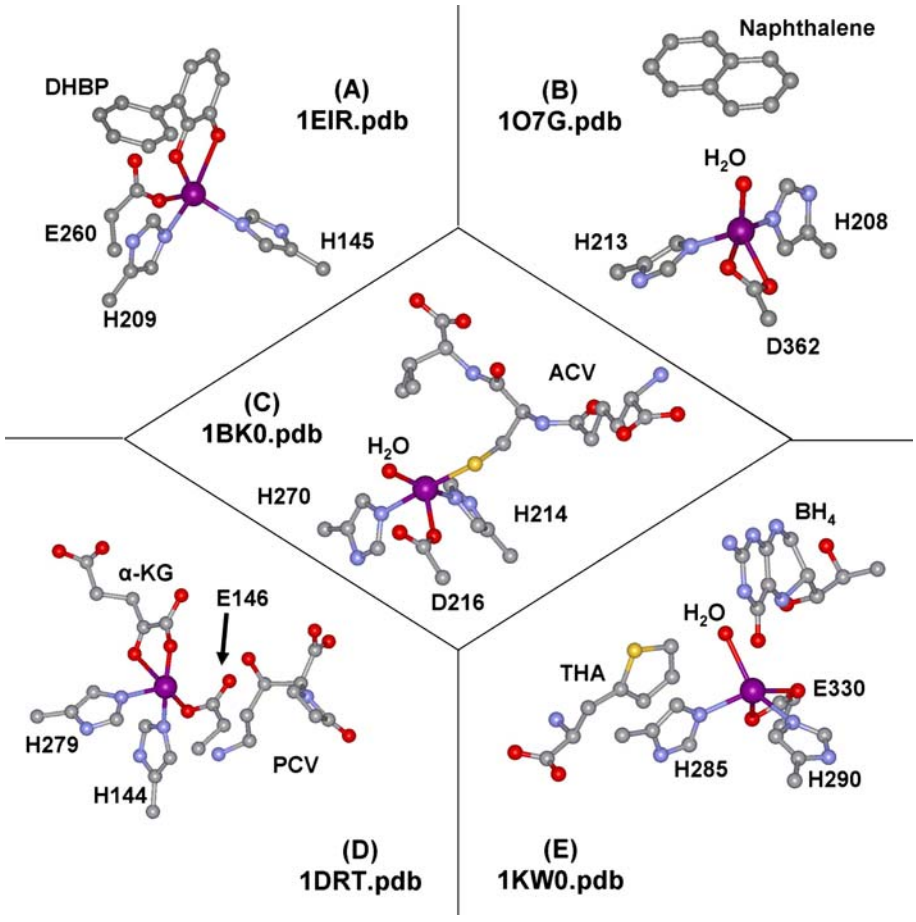

Fig. 3 Mononuclear non-heme iron enzymes containing a 2-His-1-carboxylate facial triad that have been crystallized in a state that is poised for attack by O_2. Representative members from each enzyme family include **a** the extradiol-cleaving catechol dioxygenase 2,3-dihydroxybiphenyl 1,2-dioxygenase (*BphC–DHBP*), **b** the Rieske dioxygenase naphthalene 1,2-dioxygenase (*NDO–naphthalene*), **c** isopenicillin *N* synthase (*IPNS–ACV*), **d** the α-KG dependent enzyme clavaminate synthase (*CAS–α-KG–PCV*), and **e** the pterin-dependent hydroxylase phenylalanine hydroxylase (*PheOH–BH_4–THA*)

three solvent molecules occupying the opposite face. At this stage, the metal center is unreactive toward dioxygen.

Examples from each enzyme family shown in Fig. 3 demonstrate that formation of an enzyme–substrate complex affects the coordination chemistry of the active site iron. For extradiol dioxygenases (i.e. 2,3-dihydroxybiphenyl 1,2-dioxygenase, BphC) and IPNS (Fig. 3a, c, respectively), their respective substrates bind directly to the iron(II) center, whereas for the α-KG dependent enzymes, such as clavaminate synthase (CAS), the cofactor α-KG coordinates to the metal center and the substrate is bound in close proximity (Fig. 3d).[1] For the Rieske dioxygenases, such as naphthalene dioxygenases (NDO), and the pterin-dependent hydroxylases, such as phenylalanine hydroxylase, neither substrate nor cofactor (in the latter case) binds directly to the metal center (Fig. 3b, e, respectively); however, in these scenarios the carboxylate of the facial triad acts as a bidentate ligand. In all five examples shown in Fig. 3, the iron center becomes five-coordinate at this stage of catalysis, a conclusion corroborated by magnetic circuilar dichroism (MCD) studies performed on a number of these enzymes [1, 3]. Substrate binding thus primes the iron active site for attack by dioxygen.

A key species in catalysis is the enzyme–substrate–(cofactor)–O_2 complex, and the crystal structure of such a species should reveal how the reactants are arranged around the metal center just prior to the initiation of turnover. To date there are three structures with an end-on bound NO serving as a surrogate for O_2 (Fig. 4), wherein NO can bind end-on *trans* to a carboxylate residue as in BphC (Fig. 4a) [37] and IPNS (Fig. 4b) [14] or *trans* to a histidine residue as in CAS (Fig. 4c) [38]. There is a structure of only one O_2 adduct available (Fig. 5), showing a side-on O_2 for NDO poised to attack the target double bond on indole [18]. These structures suggest that the 2-His-1-carboxylate facial triad provides the metal center with the flexibility to bind dioxygen in a number of modes, depending on the type of reaction to be catalyzed. This is a feature that distinguishes these non-heme iron enzymes from their heme counterparts and may account for the greater range of oxidative transformations that are catalyzed by this enzyme superfamily.

[1] A notable exception to this generalization is the case of DAOCS in which α-KG and penicillin were found in recent structures of respective binary complexes to bind in overlapping regions of the active site; it would thus appear that a ternary DAOCS–α-KG–penicillin complex could not form [36].

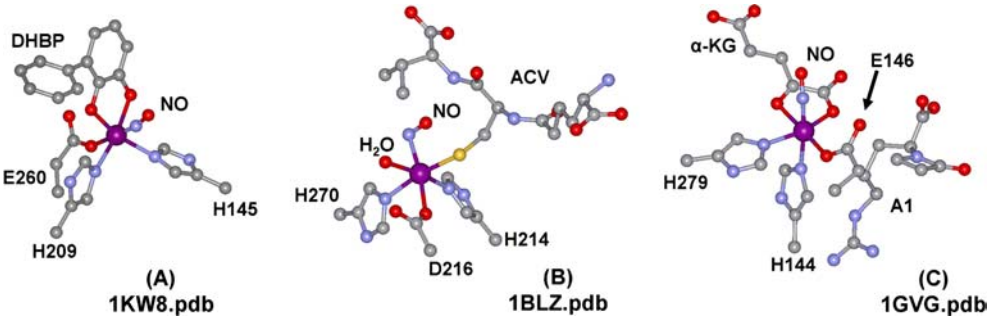

Fig. 4 Mononuclear non-heme iron enzymes containing a 2-His-1-carboxylate motif that have been crystallized in the presence of a substrate and NO (an O_2 analog) include **a** BphC (*BphC–DHBP–NO*), **b** IPNS (*IPNS–ACV–NO*), and **c** CAS (*CAS–*α*-KG–A1–NO*)

Mechanistic implications

Figure 6 shows a generalized mechanism for dioxygen-activating mononuclear non-heme iron(II) enzymes containing a 2-His-1-carboxylate motif based on the growing structural database for this superfamily and corresponding spectroscopic [1, 3] and computational [39–42] studies. The starting point is the iron(II) center of the resting enzyme that is coordinated to the facial triad on one face of its octahedral coordination sphere, with three readily displaceable ligands (shown as solvent molecules) on the opposite face (Fig. 6a). As well established by the MCD studies of Solomon and coworkers [1, 3] and supported by several crystal structures, substrate and/or cofactor binding results in the formation of a five-coordinate iron(II) center (Figs. 3, 6b) that is poised to bind O_2. For the extradiol dioxygenases, IPNS, and α-KG dependent enzymes, coordination of an anionic substrate or cofactor to the iron center is observed. The replacement of a neutral solvent molecule with an anionic ligand should decrease the Fe^{III}/Fe^{II} reduction/oxidation potential and render the iron center more susceptible to oxidation by O_2. On the other hand, for the pterin-dependent hydroxylases and Rieske dioxygenases, neither the substrate nor the electron donating cofactor coordinates to the metal center; instead the carboxylate of the facial triad becomes a bidentate ligand. It would appear that this change is sufficient to lower the barrier for O_2 binding in these active sites. Despite these differences among the five enzyme classes, the Fe–O_2 adduct in all cases does not form until the substrate and/or cofactor is present, a mechanistic strategy that helps to protect an enzyme from self-inactivation. Regardless of whether it binds near or directly to the iron(II) center, substrate binding acts as a trigger to open the sixth coordination site for O_2, thus priming the metal center for attack by dioxygen [1–3].

The next step in the proposed mechanism involves the binding of O_2 to the metal center (Fig. 6c). The crystal

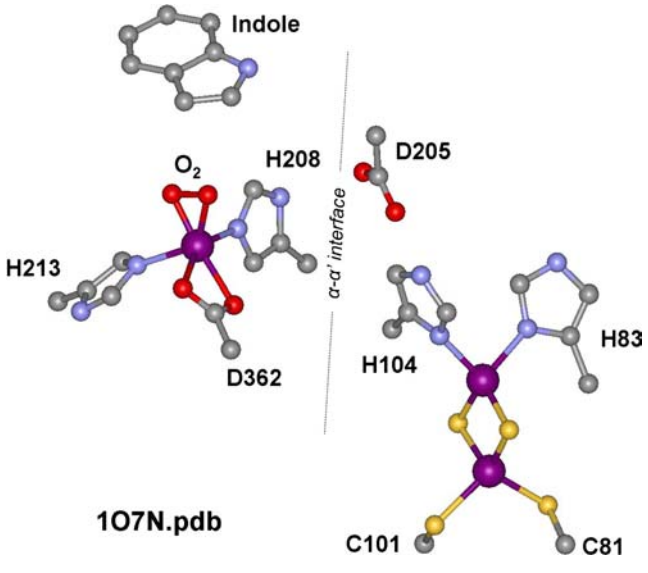

Fig. 5 The only crystallographically characterized O_2 complex of a mononuclear non-heme iron enzyme containing a 2-His-1-carboxylate facial triad is that of *NDO–indole–*O_2. Note that an aspartate residue (*D205*) connects the Rieske [2Fe–2S] center (located in a neighboring subunit) to the mononuclear iron active site

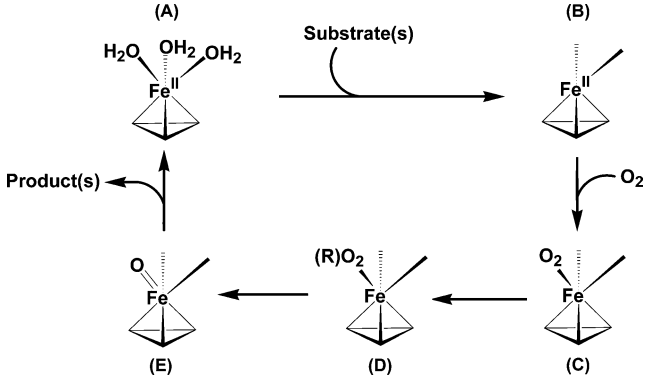

Fig. 6 A general mechanistic pathway catalyzed by a mononuclear non-heme iron enzyme containing a 2-His-1-carboxylate facial triad. **a** The iron(II) center of the resting form of the enzyme is anchored to the active site by the 2-His-1-carboxylate facial triad (depicted by the triangular base); on the opposite face are three readily displaceable ligands, depicted here as water molecules. **b** The addition of substrate displaces the sixth ligand and primes the metal center for **c** attack by O_2, which is **d** reduced to the peroxide oxidation level and **e** further activated to generate a high-valent oxidizing species. This intermediate is responsible for transforming the prime substrate into product, which is released from the active site, and **a** the resting form of the active site is subsequently regenerated. Refer to Figs. 3, 4, and 5 to view the various possible ligands that can occupy the remaining two coordination sites of the complexes depicted in **b**–**e**

structures displayed in Fig. 3 show that the 2-His-1-carboxylate facial triad can accommodate reaction schemes with molecular oxygen bound opposite to any of the three protein residues, suggesting that the identity of the *trans* ligand is not crucial for the activation of O_2. Whether the *trans* ligand may modulate the reactivity of the bound O_2 is an intriguing question that is worth investigating.

The three adjacent coordination sites available for exogenous ligand binding opposite the 2-His-1-carboxylate facial triad provide a convenient mechanism for juxtaposing dioxygen and its initial target, either the substrate itself or the cosubstrate, such that they are in the proper orientation to react. This juxtaposition is nicely illustrated in the crystal structure of the enzyme complex IPNS–δ-(L-α-aminoadipoyl)-L-cysteinyl-D-valine (ACV)–NO (Fig. 4b), where the oxygen atom of the O_2 surrogate NO is equidistant from the valine nitrogen and the cysteinyl β-carbon of the substrate ACV, from which two hydrogen atoms are abstracted and between which a bond forms. This mechanistic feature is also utilized by extradiol dioxygenases (Fig. 4a) and α-KG dependent enzymes (Fig. 4c), thereby providing a convenient mechanism for O_2 reduction by substrate or cofactor. Although neither substrate nor cofactor binds to the iron center of the pterin-dependent hydroxylases, BH_4 is close enough to the iron center to form an iron–O_2–pterin intermediate, which is analogous to the intermediates proposed for extradiol dioxygenases, IPNS, and α-KG dependent enzymes. In the case of the Rieske dioxygenases, it is proposed that O_2 binding to the iron(II) center is followed immediately by electron transfer from the nearby reduced Rieske [2Fe–2S] cluster to generate an $Fe^{III}(\eta^2\text{–}O_2)$ species [18]. This species is the only dioxygen-bound intermediate in the superfamily to be crystallographically observed thus far (Fig. 5). Whatever the mechanistic details, O_2 is reduced to the peroxide oxidation level (Fig. 6d) at this stage of the mechanism in all enzyme classes.

O–O bond cleavage occurs in the next step of the mechanistic pathway. For the extradiol and Rieske dioxygenases, substrate oxidation may occur either directly from the peroxo intermediate or via prior cleavage of the O–O bond to form a high-valent intermediate. Independent density functional theory (DFT) calculations support one scenario or the other for the extradiol-cleaving dioxygenases [39, 41], but direct mechanistic evidence is lacking. For the Rieske dioxygenases, DFT calculations favor direct attack by the iron(III)-side-on-peroxo species owing to the high energy calculated for the putative $HO\text{–}Fe^{V}=O$ intermediate [40], a species that is related to the active species in related OsO_4, RuO_4, and MnO_4^- systems known to effect *cis*-dihydroxylation of olefins [43–45]. However, there is some experimental evidence in favor of prior O–O bond cleavage to form an oxoiron(V) oxidant. It has been reported that ^{18}O from $H_2^{18}O$ is incorporated into the indanol product formed by the hydroxylation of indane by toluene dioxygenases [5]; this observation requires an oxidant capable of ^{18}O exchange with water. So the involvement of high-valent iron-oxo species is uncertain in these two enzyme classes.

On the other hand, oxoiron(IV) intermediates are implicated from substrate analogue studies for IPNS [13], α-KG dependent enzymes [8], and pterin-dependent hydroxylases [7] (Fig. 6e) as the species responsible for attacking the prime substrate and transforming it into product. Direct evidence for a high-valent iron intermediate has recently been obtained for the α-KG dependent enzyme taurine/α-KG dioxygenases (TauD). A high-spin oxoiron(IV) center with a UV absorption near 320 nm has been trapped in the reaction of the TauD–α-KG–taurine complex with O_2 and characterized by Mössbauer ($\Delta E_Q = -0.88$ mm/s and $\delta = 0.31$ mm/s) [46], resonance Raman ($\nu_{Fe=O} = 821$ cm^{-1}) [47], and extended X-ray absorption fine structure ($r_{Fe=O} = 1.62$ Å) [48] techniques. Furthermore, the rate of decay of this intermediate is strongly retarded by deuterium isotope substitution of the target C–H bond (kinetic isotope effect approximately 28–50) [49]. Thus, by extension, the oxoiron(IV) species is postulated to be the oxidant in many of the diverse transformations carried out by this superfamily of enzymes.

The properties of the oxoiron(IV) intermediate of TauD can be compared with those of synthetic oxoiron(IV) complexes that have been characterized within the same time frame [50–55], including one that has been characterized crystallographically [50]. Interestingly, the TauD intermediate shares similar $\nu_{Fe=O}$ and $r_{Fe=O}$ values with the model complexes, but the TauD intermediate is high-spin iron(IV), while all the synthetic complexes are low-spin. DFT studies suggest that the ground-state bonding properties of the Fe=O bond should not be greatly affected by spin state [56], in agreement with the experimental results, but more work needs to be done to uncover subtleties that may affect the reactivity of the oxoiron(IV) center.

Perspective

Over the past few years the number of structurally characterized enzymes containing an iron center bound by the 2-His-1-carboxylate facial triad has grown dramatically. Members of this superfamily of enzymes continue to be found throughout aerobic life and are responsible for carrying out an impressive array of transformations that require dioxygen activation. The observation of Fe–O_2 [18] and $Fe^{IV}=O$ [46] intermediates for two of these enzymes, coupled with corresponding advances in trapping synthetic intermediates [2], represent a significant step forward toward understanding the mechanisms of dioxygen activation by this superfamily. However, for almost all of the 2-His-1-carboxylate iron enzymes, the nature of the oxidizing species remains unproven and, in some cases, enigmatic at best. As studies of these enzymes progress, we expect

to see common threads in the mechanisms for dioxygen activation. Undoubtedly, these mechanistic insights will help define how one of nature's recurring metal binding motifs is able to promote dioxygen activation for a variety of reactions.

References

1. Solomon EI, Brunold TC, Davis MI, Kemsley JN, Lee S-K, Lehnert N, Neese F, Skulan AJ, Yang Y-S, Zhou J (2000) Chem Rev 100:235–349
2. Costas M, Mehn MP, Jensen MP, Que L Jr (2004) Chem Rev 104:939–986
3. Solomon EI, Decker A, Lehnert N (2003) Proc Natl Acad Sci USA 100:3589–3594
4. Bugg TDH (2003) Tetrahedron 59:7075–7101
5. Wackett LP (2002) Enzyme Microb Tech 31:577–587
6. Vaillancourt FH, Bolin JT, Eltis LD (2004) In: Ramos J-L (ed) Pseudomonas. Kluwer/Plenum, New York, pp 359–395
7. Fitzpatrick PF (2003) Biochemistry 42:14083–14091
8. Hausinger RP (2004) Crit Rev Biochem Mol Biol 39:21–68
9. Schofield CJ, Zhang Z (1999) Curr Opin Struct Biol 9:722–731
10. Sono M, Roach MP, Coulter ED, Dawson JH (1996) Chem Rev 96:2841–2887
11. Han S, Eltis LD, Timmis KN, Muchmore SW, Bolin JT (1995) Science 270:976–980
12. Senda T, Sugiyama K, Narita H, Yamamoto T, Kimbara K, Fukuda M, Sato M, Yano K, Mitsui Y (1996) J Mol Biol 255:735–752
13. Roach PL, Clifton IJ, Fülöp V, Harlos K, Barton GJ, Hajdu J, Andersson I, Schofield CJ, Baldwin JE (1995) Nature 375:700–704
14. Roach PL, Clifton IJ, Hensgens CMH, Shibata N, Schofield CJ, Hajdu J, Baldwin JE (1997) Nature 387:827–830
15. Valegård K, van Scheltinga ACT, Lloyd MD, Hara T, Ramaswamy S, Perrakis A, Thompson A, Lee H-J, Baldwin JE, Schofield CJ, Hajdu J, Andersson I (1998) Nature 394:805–809
16. Zhang Z, Ren J, Stammers DK, Baldwin JE, Harlos K, Schofield CJ (2000) Nat Struct Biol 7:127–133
17. Kauppi B, Lee K, Carredano E, Parales RE, Gibson DT, Eklund H, Ramaswamy S (1998) Structure 6:571–586
18. Karlsson A, Parales JV, Parales RE, Gibson DT, Eklund H, Ramaswamy S (2003) Science 299:1039–1042
19. Flatmark T, Stevens RC (1999) Chem Rev 99:2137–2160
20. Zhang Z, Ren J-s, Clifton IJ, Schofield CJ (2004) Chem Biol 11:1383–1394
21. Hegg EL, Que L Jr (1997) Eur J Biochem 250:625–629
22. Que L Jr (2000) Nat Struct Biol 7:182–184
23. Schofield CJ, Baldwin JE, Byford MF, Clifton I, Hajdu J, Hensgens C, Roach P (1997) Curr Opin Struct Biol 7:857–864
24. Rocklin AM, Tierney DL, Kofman V, Brunhuber NMW, Hoffman BM, Christoffersen RE, Reich NO, Lipscomb JD, Que L Jr (1999) Proc Natl Acad Sci USA 96:7905–7909
25. Zhou J, Rocklin AM, Lipscomb JD, Que L Jr, Solomon EI (2002) J Am Chem Soc 124:4602–4609
26. Rocklin AM, Kato K, Liu H-w, Que L Jr, Lipscomb JD (2004) J Biol Inorg Chem 9:171–182
27. Liu P, Liu A, Yan F, Wolfe MD, Lipscomb JD, Liu H-w (2003) Biochemistry 42:11577–11586
28. Liu P, Mehn MP, Yan F, Zhao Z, Que L Jr, Liu H-w (2004) J Am Chem Soc 126:10306–10312
29. Eltis LD, Bolin JT (1996) J Bacteriol 178:5930–5937
30. Spence EL, Kawamukai M, Sanvoisin J, Braven H, Bugg TDH (1996) J Bacteriol 178:5249–5256
31. Jiang H, Parales RE, Lynch NA, Gibson DT (1996) J Bacteriol 178:3133–3139
32. Prescott AG (1993) J Exp Bot 44:849–861
33. Borovok I, Landman O, Kreisberg-Zakarin R, Aharonowitz Y, Cohen G (1996) Biochemistry 35:1981–1987
34. Tan DSH, Sim T-S (1996) J Biol Chem 271:889–894
35. Kappock TJ, Caradonna JP (1996) Chem Rev 96:2659–2756
36. Valegård K, van Scheltinga ACT, Dubus A, Ranghino G, Öster LM, Hajdu J, Andersson I (2004) Nat Struct Mol Biol 11:95–101
37. Sato N, Uragami Y, Nishizaki T, Takahashi Y, Sazaki G, Sugimoto K, Nonaka T, Masai E, Fukuda M, Senda T (2002) J Mol Biol 321:621–636
38. Zhang Z, Ren J-s, Harlos K, McKinnon CH, Clifton IJ, Schofield CJ (2002) Febs Lett 517:7–12
39. Deeth RJ, Bugg TDH (2003) J Biol Inorg Chem 8:409–418
40. Bassan A, Blomberg MRA, Siegbahn PEM (2004) J Biol Inorg Chem 9:439–452
41. Siegbahn PEM, Haeffner F (2004) J Am Chem Soc 126:8919–8932
42. Bassan A, Borowski T, Siegbahn PEM (2004) Dalton Trans 20:3153–3162
43. Schröder M (1980) Chem Rev 80:187–213
44. Shing TKM, Tam EKW, Tai VW-F, Chung IHF, Jiang Q (1996) Chem Eur J 2:50–57
45. Lee DG, Chen T (1989) J Am Chem Soc 111:7534–7538
46. Price JC, Barr EW, Tirupati B, Bollinger JM Jr, Krebs C (2003) Biochemistry 42:7497–7508
47. Proshlyakov DA, Henshaw TF, Monterosso GR, Ryle MJ, Hausinger RP (2004) J Am Chem Soc 126:1022–1023
48. Riggs-Gelasco PJ, Price JC, Guyer RB, Brehm JH, Barr EW, Bollinger JM Jr, Krebs C (2004) J Am Chem Soc 126:8108–8109
49. Price JC, Barr EW, Glass TE, Krebs C, Bollinger JM Jr (2003) J Am Chem Soc 125:13008–13009
50. Rohde J-U, In J-H, Lim MH, Brennessel WW, Bukowski MR, Stubna A, Münck E, Nam W, Que L Jr (2003) Science 299:1037–1039
51. Lim MH, Rohde J-U, Stubna A, Bukowski MR, Costas M, Ho RYN, Münck E, Nam W, Que L Jr (2003) Proc Natl Acad Sci USA 100:3665–3670
52. Kaizer J, Costas M, Que L Jr (2003) Angew Chem Int Ed 42:3671–3673
53. Kaizer J, Klinker EJ, Oh NY, Rohde J-U, Song WJ, Stubna A, Kim J, Münck E, Nam W, Que L Jr (2004) J Am Chem Soc 126:472–473
54. Balland V, Charlot M-F, Banse F, Girerd J-J, Mattioli TA, Bill E, Bartoli J-F, Battioni P, Mansuy D (2004) Eur J Inorg Chem 301–308
55. Rohde J-U, Torelli S, Shan X, Lim MH, Klinker EJ, Kaizer J, Chen K, Nam W, Que L Jr (2004) J Am Chem Soc 126:16750–16761
56. Decker A, Rohde J-U, Que L Jr, Solomon EI (2004) J Am Chem Soc 126:5378–5379
57. Sugimoto K, Senda T, Aoshima H, Masai E, Fukuda M, Mitsui Y (1999) Structure 7:953–965
58. Titus GP, Mueller HA, Burgner J, de Córdoba SR, Peñalva MA, Timm DE (2000) Nat Struct Biol 7:542–546
59. Serre L, Sailland A, Sy D, Boudec P, Rolland A, Pebay-Peyroula E, Cohen-Addad C (1999) Structure 7:977–988
60. Goodwill KE, Sabatier C, Marks C, Raag R, Fitzpatrick PF, Stevens RC (1997) Nat Struct Biol 4:578–585
61. Kobe B, Jennings IG, House CM, Michell BJ, Goodwill KE, Santarsiero BD, Stevens RC, Cotton RGH, Kemp BE (1999) Nat Struct Biol 6:442–448
62. Erlandsen H, Kim JY, Patch MG, Han A, Volner A, Abu-Omar MM, Stevens RC (2002) J Mol Biol 320:645–661